PHYSICAL REVIEW D VOLUME 16, NUMBER 1 1 JULY 1977

Isobar formalism and one-pion-exchange partial-wave cross sections in $\pi N \rightarrow \pi\pi N$ †

Ronald Aaron
Northeastern University, Boston, Massachusetts 02115

R. D. Amado
University of Pennsylvania, Philadelphia, Pennsylvania 19174

Richard A. Arndt,* Yogesh Goradia,* Doris C. Teplitz, and Vigdor L. Teplitz
Virginia Polytechnic Institute and State University, Blacksburg, Virginia 24061
(Received 22 November 1976)

This work is a prelude to a phase-shift analysis of $\pi N \rightarrow \pi\pi N$ which we are presently performing. We here review the partial-wave isobar formalism for the above process and introduce the notation being used in our analysis. We compute the partial-wave projections of the one-pion-exchange diagrams because we hope to use the *high-partial-wave contributions* of these diagrams, which are not modified by the interactions, to remove phase ambiguities in the partial waves being varied. A study of the low partial waves, even though they violate unitarity badly, gives modest insights into the results of previous partial-wave analyses.

I. INTRODUCTION

Single-pion production at intermediate energies is an important source of information concerning meson-baryon resonances. One can obtain from its analysis partial widths of known resonances and, perhaps, discover new resonances that might be difficult to identify in an elastic phase-shift analysis. Recent theoretical advances have generated considerable interest in this process. In particular, a proposed connection between current and constituent quarks[1] can be tested through the magnitudes and signs of amplitudes for pionic transitions between hadrons.[2] Equivalently, modified versions of $SU(6)_W$ classify baryon resonances and at the same time predict amplitudes for reactions of the type

$$\begin{aligned} &\pi N \rightarrow \epsilon N ,\\ &\pi N \rightarrow \rho N ,\\ &\pi N \rightarrow \pi N , \end{aligned} \tag{1.1}$$

etc.[3] From the experimental side, $\pi N \rightarrow \pi\pi N$ data in the region up to 1 GeV above threshold have grown in abundance to the point where they may be able to support detailed partial-wave decomposition. Such an analysis has recently been performed by a Berkeley-SLAC collaboration (BSC)[4] in the framework of the standard isobar model.[5] Their fit began with the 60 partial waves with final orbital angular momentum ≤ 3 for the quasi-two-body processes described by (1.1). The BSC result was a fit with 28 of the 60 partial waves.

Our collaboration is preparing for an expanded analysis of an enlarged data set. We hope to include two important *new* features in our fitting procedure. First, we shall incorporate unitarity and analyticity into the isobar model. In general, this modification results in subenergy dependence of amplitudes assumed to be constant in the standard isobar model.[6,7] A simplified version of the methods we shall use has already been applied to an analysis of the three-pion system[8]; we shall discuss this subject in more detail in another note. The second new feature, which we shall discuss here, is the use of the one-pion-exchange (OPE) diagram in the fitting procedure. In 1958 Chew and Low[9] suggested that OPE could dominate $\pi N \rightarrow \pi\pi N$ in certain kinematic regions and many other authors[10] have persued the idea since then. We propose the inclusion of the higher partial waves from OPE as background in the fitting amplitude as a method of removing the overall phase ambiguity in the partial waves being varied, as well as to account for the peripheral part of the amplitude. The procedure recommended is, of course, analogous to that used in obtaining the pion-nucleon coupling constant and the low-partial-wave amplitudes from low-energy nucleon-nucleon scattering.[11] For example, if we were dealing with spinless particles, we would expand an isobar amplitude $F(p^2, q^2, \cos\theta)$ in the form

$$\begin{aligned} F(p^2,q^2,\cos\theta) = \sum_{l=0}^{l_{\max}} (2l+1) f_l(p^2,q^2) P_l(\cos\theta) \\ + \Big[B(p^2,q^2,\cos\theta) \\ - \sum_{l=0}^{l_{\max}} (2l+1) b_l(p^2,q^2) P_l(\cos\theta) \Big] . \end{aligned} \tag{1.2}$$

In (1.2) above, B and b are the Born approximations of F and f, respectively, and we have explicitly assumed that for $l \geq l_{\max}$, the partial-wave amplitudes f_l are not modified by the interactions and may be replaced by their Born approximations. In the nucleon-nucleon case, $l_{\max}$ was one of the fitting parameters; $\pi N \rightarrow \pi\pi N$ is a much larger problem, and the parameters equivalent to $l_{\max}$ cannot be varied. Instead, we shall use the methods of the Appendix to determine at which point one may replace the partial-wave amplitudes f_l by b_l.

A detailed description of our version of the isobar model is given in Sec. II. In Sec. III we give expressions for the partial-wave OPE projections and for the contributions of each partial wave to the cross section. [See Eqs. (3.14) and (3.27).] In Sec. IV we calculate numerically the contribution of each separate OPE partial wave and compare the results with the contributions BSC find from their fit to the data. An interesting discrepancy is observed in the case of the *PPIJ* ρ waves. Some preliminary results showing the effects of including analyticity and unitarity are discussed in the Appendix.

II. ISOBAR MODEL

Before discussing the isobar model we first give a brief review of the conventions. Following Pilkuhn[12] (or Bjorken and Drell[13]) we define the transition (T) matrix in terms of the S matrix by

$$S_{fi} = \delta_{fi} + (2\pi)^4 i\delta^4(P_f - P_i)T_{fi}, \tag{2.1}$$

where the unitarity statement is

$$SS^\dagger = S^\dagger S = 1. \tag{2.2}$$

We are using the normalization convention

$$\langle p | p' \rangle = (2\pi)^4\delta^4(p - p'), \tag{2.3}$$

and thus the n-body phase-space element is given by

$$d\rho^{(n)} = (2\pi)^4\delta^4\left(P_f - \sum_{i=1}^{n} q_i\right)\left(\prod_{A,\,i=1}^{N_A} N_A!\right)^{-1} \prod_{i=1}^{n} (2\pi)^{-4}\eta_i d^4q_i 2\pi\delta^+(q_i^2 - m_i^2), \tag{2.4}$$

where N_A is the number of identical particles of type A,

$$\delta^+(q_i^2 - m_i^2) = \theta(q_{i0})\delta(q_i^2 - m_i^2), \tag{2.5}$$

and for bosons $\eta_i = 1$, while for fermions $\eta_i = 2m_i$.

Working in the overall center-of-mass (c.m.) system, the total cross section $\sigma(t_1, t_2, t_3; t_\pi, t_N)$ for the reaction $\pi(-\vec{p}, t_\pi) + N(\vec{p}, s, t_N) \rightarrow \pi(\vec{p}_1, t_1) + \pi(\vec{p}_2, t_2) + N(\vec{p}_3, r, t_3)$ may be written

$$\sigma(t_1, t_2, t_3; t_N t_\pi) = M(4pW)^{-1} \sum_{s,\,r} \int d\rho^{(3)} |\langle \vec{p}_1 t_1, \vec{p}_2 t_2, \vec{p}_3 r t_3 | T | \vec{p}, s t_N t_\pi \rangle|^2, \tag{2.6}$$

where M is the nucleon mass and W is the c.m. energy. In Eq. (2.6) s and r are the z components of the nucleon spins and the t's are the third components of particle isospins. The usual Feynman rules[14] are used in constructing matrix elements such as $\langle T \rangle$. Integrals over phase space are evaluated using Eq. (2.4) with no additional factors.

The isobar model is defined by choosing a particular form for the T-matrix element in Eq. (2.6). It is assumed to factor into a part describing production of a particle and correlated pair (isobar) from the initial pion-nucleon state, and another part describing the propagation and subsequent decay of the isobar. For example, considering only the ϵ, ρ, and $\Delta(1236)$ isobars and for a given total isotopic spin I we write

$$\langle \vec{p}_1 t_1, \vec{p}_2 t_2, \vec{p}_3 t_3 | T^I | \vec{p}, s t_N t_\pi \rangle = T_\epsilon^I + T_\rho^I + T_\Delta^I(1) + T_\Delta^I(2), \tag{2.7}$$

with the arguments 1 and 2 of T_Δ^I referring to the spectator pion:

$$T_\epsilon^I = \langle \vec{p}_3 r | f_\epsilon^I | \vec{p} s \rangle W_3 \frac{e^{i\delta_\epsilon(q_{12})} \sin\delta_\epsilon(q_{12})}{q_{12}} \langle i_3 i_\epsilon t_3 t_\epsilon | IT \rangle \langle i_1 i_2 t_1 t_2 | i_\epsilon t_\epsilon \rangle \langle i_N i_\pi t_N t_\pi | IT \rangle. \tag{2.8}$$

In Eq. (2.8) above and from this point on we adopt the convention of BSC that in any Clebsch-Gordan[15] coefficient the fermion always appears first. Continuing, we have

$$T_\rho^I = \sum_\mu \langle \vec{p}_3 r \mu | f_\rho^I | \vec{p} s \rangle W_3 \frac{e^{i\delta_\rho(q_{12})} \sin\delta_\rho(q_{12})}{q_{12}^3} V_\mu(\vec{p}_1, \vec{p}_2) \langle i_3 i_\rho t_3 t_\rho | IT \rangle \langle i_1 i_2 t_1 t_2 | i_\rho t_\rho \rangle \langle i_N i_\pi t_N t_\pi | IT \rangle, \tag{2.9}$$

$$T^I_\Delta(1)=\sum_\mu \langle \vec{p}_1\mu\,|\,f^I_\Delta\,|\vec{p}s\rangle\,W_1\,\frac{e^{i\delta_\Delta(q_{23})}\sin\delta_\Delta(q_{23})}{q_{23}^{\;3}}\,\Delta_\mu(\vec{p}_2\vec{p}_3r)\,\langle i_\Delta\,i_1t_\Delta t_1\,|IT\rangle\langle i_3i_2t_3t_2\,|\,i_\Delta t_\Delta\rangle\langle i_N\,i_\pi\,t_N\,t_\pi\,|IT\rangle\,, \tag{2.10}$$

$$T^I_\Delta(2)=T^I_\Delta(1)\text{ with }1\rightleftarrows 2\,, \tag{2.11}$$

where

$$W_i^{\;2}=W^2-2W\omega_i+m_i^{\;2}\,,\qquad \omega_i=(p_i^{\;2}+m_i^{\;2})^{1/2}\,. \tag{2.12}$$

In Eqs. (2.8)–(2.11) q_{ij} is the magnitude of the three-momentum of particle i or j in their own c.m. system; δ_ϵ is the $I=0$, $J=0$ π-π phase shift, δ_ρ is the $I=1$, $J=1$ π-π phase shift, and δ_Δ is the $I=\frac{3}{2}$, $J=\frac{3}{2}$ π-N phase shift. The functions V_μ and Δ_μ are spin wave functions of the ρ and Δ mesons, respectively,[16] where μ is the z component of spin—the function V_μ shall be discussed in more detail below.

We now expand Eqs. (2.8)–(2.11) in partial-wave amplitudes which will contain the fitting parameters of the analysis:

$$\langle\vec{p}_3r\,|\,f^I_\epsilon\,|\vec{p}s\rangle=\sum_{\substack{J,M\\ l',m',l,m}}[(v_{l'})^{1/2}/R_{\epsilon,l'}]f^I_\epsilon(J,l',l)\langle l'\tfrac{1}{2}m'r\,|JM\rangle\,Y_{l'm'}(\hat{p}_3)Y_{lm}(\hat{p})\langle l\,\tfrac{1}{2}ms\,|JM\rangle\,, \tag{2.13}$$

$$\langle\vec{p}_3r\mu\,|\,f^I_\rho\,|\vec{p}s\rangle=\sum_{\substack{J,M,l',m'\\ l,m,j,m_j}}[(v_{l'})^{1/2}/R_{\rho,l'}]f^I_\rho(J,j,l',l)\langle\tfrac{1}{2}\,1r\mu\,|\,jm_j\rangle\langle l'jm'm_j\,|JM\rangle Y_{l'm'}(\hat{p}_3)Y_{lm}(\hat{p})\langle l\,\tfrac{1}{2}ms\,|JM\rangle\,, \tag{2.14}$$

$$\langle\vec{p}_1\mu\,|\,f^I_\Delta\,|\vec{p}s\rangle=\sum_{\substack{J,M\\ l',m',l,m}}[(v_{l'})^{1/2}/R_{\Delta,l'}]f^I_\Delta(J,l',l)\langle l'\tfrac{3}{2}m'\mu\,|JM\rangle Y_{l'm'}(\hat{p}_1)Y_{lm}(\hat{p})\langle l\,\tfrac{1}{2}ms\,|JM\rangle\,, \tag{2.15}$$

where we have suppressed momenta momenta in the partial-wave amplitudes. The functions $v_{l'}$ are barrier-penetration factors defined by Blatt and Weisskopf[17]; these factors have rapid dependence on the isobar mass (subenergy). Having explicitly removed them, one may hope that the remaining factors in the partial-wave amplitudes, f^I_ϵ, f^I_ρ, f^I_Δ, etc., are slowly varying functions of subenergy and may, perhaps, be approximated by constants for fixed total center-of-mass energy W. In the BSC analysis it is the f's which are taken as the constant fitting parameters at fixed W. The normalization factors R in Eqs. (2.13)–(2.15) are given by

$$R_{\epsilon,l'}^{\;2}=h(W)\int_{2\mu}^{W-M}p_3W_3^{\;2}dW_3\,\frac{\sin^2\delta_\epsilon(q_{12})}{q_{12}}\,v_{l'}\,, \tag{2.16}$$

$$R_{\rho,l'}^{\;2}=\frac{h(W)}{3}\int_{2\mu}^{W-M}p_3W_3^{\;2}dW_3\,\frac{\sin^2\delta_\rho(q_{12})}{q_{12}^{\;3}}\,v_{l'}\,, \tag{2.17}$$

$$R_{\Delta,l'}^{\;2}=\frac{h(W)}{3}\int_{M+\mu}^{W-\mu}p_1W_1^{\;2}dW_1\,\frac{\sin^2\delta_\Delta(q_{12})}{q_{12}^{\;3}}\,v_{l'}\,, \tag{2.18}$$

where

$$h(W)=\frac{1}{32}\left(\frac{M}{W}\right)^2\frac{p}{(2\pi)^6}\,. \tag{2.19}$$

With this choice of normalization, in a given isospin channel I, the cross section of Eq. (2.6) in terms of the partial-wave coefficients takes the form

$$\begin{aligned}\sigma^I=\frac{4\pi}{p^2}\sum_{J,j,l',l}(J+\tfrac{1}{2})\bigg\{&\frac{h(W)}{R_{\epsilon,l'}^{\;2}}\int_{2\mu}^{W-M}p_3W_3^{\;2}dW_3\,\frac{\sin^2\delta_\epsilon(q_{12})}{q_{12}}\,|\,f^I_\epsilon(J,l',l)\,|^2v_{l'}\\ &+\frac{h(W)}{3R_{\rho,l'}}\int_{2\mu}^{W-M}p_3W_3^{\;2}dW_3\,\frac{\sin^2\delta_\rho(q_{12})}{q_{12}^{\;3}}\,|\,f^I_\rho(J,j,l',l)\,|^2v_{l'}\\ &+\frac{2h(W)}{3R_{\Delta,l'}^{\;2}}\int_{M+\mu}^{W-\mu}p_1W_1^{\;2}dW_1\,\frac{\sin^2\delta_\Delta(q_{23})}{q_{23}^{\;3}}\,|\,f^I_\Delta(J,l',l)\,|^2v_{l'}+\text{overlap integrals}\bigg\}.\end{aligned} \tag{2.20}$$

In the above equation the overlap integrals contain phase-space integrations over products of amplitudes $f^*_\epsilon f_\Delta$, etc.; these are discussed in detail elsewhere.[18] The normalization factors R_ϵ, R_ρ, and R_Δ have been chosen so that in the zero-width limit Eq. (2.6) yields

$$\sigma^I = \frac{4\pi}{p^2} \sum_{J,j,l',l} (J+\tfrac{1}{2})\{|f_\epsilon^I(J,l',l)|^2 + |f_\rho^I(J,j,l',l)|^2 + 2|f_\Delta(J,l',l)|^2\}, \tag{2.21}$$

and the partial-wave amplitudes f_ϵ, f_ρ, and f_Δ can thus be identified as those amplitudes which BSC plot on their Argand diagrams. In general, for finite-width resonances the f's are complicated functions of the isobar mass [W_i of Eq. (2.12)].

III. ONE-PION EXCHANGE

We now calculate the contributions of the one-pion-exchange diagram (shown schematically in Fig. 1) to the partial-wave amplitudes f_ϵ^I and f_ρ^I of Sec. II. This contribution is given by standard Feynman rules as[14]

$$\frac{g\bar{u}_r(\vec{p}_3)\gamma_5\tau_{t_2}u(\vec{p}'')\mathfrak{M}_{1,2\to 1',2'}}{\mu^2 - t}, \quad t=(p''-p_3)^2 \tag{3.1}$$

with $g^2/4\pi \cong 15$ and

$$\mathfrak{M}_{1,2\to 1',2'} = -\sum_{i',l} \mathcal{P}_{i'}(2l+1)[32\pi(s_{\pi\pi}/(s_{\pi\pi}-4\mu^2))^{1/2}\exp(i\delta_{\pi\pi}^{l,i'})\sin\delta_{\pi\pi}^{l,i'}]P_l(z_{\pi\pi}), \tag{3.2}$$

where $s_{\pi\pi}$ is the square of the c.m. energy of the $\pi\pi$ system, $z_{\pi\pi}$ is the cosine of the c.m. scattering angle, and the $\mathcal{P}_{i'}$ are $\pi\pi$ isospin projection operators. We keep here only the $i'=l=0$ (ϵ) and $i'=l=1$ (ρ) contributions to the sum in Eq. (3.2). The isospin content of Eq. (3.1) is expressed by the matrix element

$$\langle t_1't_2't_3|\tau_{t_2}\mathcal{P}_{i'}|t''t_1\rangle = \langle t_1't_2'|\mathcal{P}_{i'}|t_1t_2\rangle\langle t_3|\tau_{t_2}|t''\rangle, \tag{3.3}$$

which may be expanded in terms of states of definite total isospin I and third component M. The expansion coefficients form a unitary matrix whose elements are Clebsch-Gordan coefficients. We thus write

$$\langle t_1't_2't_3|\tau_{t_2}\overline{\mathcal{P}}_{i'}|t''t_1\rangle = \sum_I \langle\tfrac{1}{2}1t''t_1|IM\rangle\langle 11t_1't_2'|i't'\rangle\langle\tfrac{1}{2}i't_3t'|IM\rangle\langle IMi'|\tau_{t_2}|IM1\rangle. \tag{3.4}$$

Using the Wigner-Eckart theorem,[19]

$$\langle t_3|\tau_{t_2}|t''\rangle = \sqrt{3}\exp(it_2\varphi)\langle\tfrac{1}{2}1t_3t_2|\tfrac{1}{2}t''\rangle, \tag{3.5}$$

and expanding in states of total isospin we obtain

$$\langle t_1't_2'|\mathcal{P}_i|t_1t_2\rangle = \langle 11t_1't_2'|i't'\rangle\langle 11t_1t_2|i't'\rangle; \tag{3.6}$$

substituting (3.5) and (3.6) in the right-hand side of Eq. (3.3), with the choice $\varphi=0$, we now obtain

$$\langle t_1't_2't_3|\tau_{t_2}\mathcal{P}_{i'}|t''t_1\rangle = \sqrt{3}\langle\tfrac{1}{2}1t_3t_2|\tfrac{1}{2}t''\rangle\langle 11t_1't_2'|i't'\rangle\langle 11t_1t_2|i't'\rangle. \tag{3.7}$$

Comparing (3.4) and (3.7), multiplying by the appropriate Clebsch-Gordan coefficients, and summing over third components, we have the result

$$\langle IMi|\tau_{t_2}|IM1\rangle = \sqrt{3}\sum_{\mu_1\mu_3}\langle\tfrac{1}{2}1t_3t_2|\tfrac{1}{2}t''\rangle\langle 11t_1t_2|i't'\rangle\langle\tfrac{1}{2}1t''t_1|IM\rangle\langle\tfrac{1}{2}i't_3t'|IM\rangle \equiv \sqrt{3}\,\chi_{i'}^I,$$

$$\chi_{i'}^I = (-1)^{i'}[2(2i'+1)]^{1/2}W(1I1\tfrac{1}{2};\tfrac{1}{2}i'), \tag{3.8}$$

where W is a Racah coefficient and the notation has been chosen for its consistency with that of Rose.[15] We shall hereafter refer to $\chi_{i'}^I$ as an isospin recoupling coefficient. We have been careful to use a Baryon-first convention in our Clebsch-Gordan coefficients and thus our result for the recoupling coefficient is identical to that of BSC. For $I=\frac{1}{2}$, $\chi_\epsilon=-1/\sqrt{3}$ and $\chi_\rho=-\sqrt{2/3}$; for $I=\frac{3}{2}$, $\chi_\rho=+1/\sqrt{6}$.

Comparing Eqs. (2.8) and (3.1) we have

$$\langle\vec{p}_3r|b_\epsilon^I|\vec{p}s\rangle = \sqrt{3}\chi_\epsilon^I 16\pi g\bar{u}_r(\vec{p}_3)\gamma_5u_s(\vec{p})(\mu^2-t)^{-1}, \tag{3.9}$$

where we have replaced f_ϵ^I of Eq. (2.8) by its Born approximation b_ϵ^I. We now calculate $\pi N\to\epsilon N$ "cross sections" for each partial wave using Eq. (2.20) without the overlap integrals, together with the partial-wave expansion Eq. (2.13). The partial-wave functions $b^I(J,l',l)$ normalized to the BSC Argand diagrams are obtained by projecting

$$R_{\epsilon,l'}^{-1}(v_{l'})^{1/2} b_\epsilon^I(J,l',l) = \sum_{\substack{m,m'\\r,s}} \int d\Omega_{\hat p_3} \int d\Omega_{\hat p} \langle l'\tfrac12 m' r|JM\rangle Y^*_{l'm'}(\hat p_3)\langle \vec p_3 r|b_\epsilon^I|\vec p s\rangle Y_{lm}(\hat p)\langle l\tfrac12 ms|JM\rangle . \tag{3.10}$$

Using the relation

$$\langle r|\vec\sigma\cdot\vec k|s\rangle = \sum_\mu \sqrt3\,\langle \tfrac12 1 s\mu|\tfrac12 r\rangle k_\mu^* , \tag{3.11}$$

the integrals over solid angles and sums over Clebsch-Gordan coefficients can be evaluated to yield

$$R_{\epsilon,l'}^{-1}(v_{l'})^{1/2} b_\epsilon^I(J,l',l) = C^I_{\epsilon,l'}[6(2l+1)]^{1/2}\langle l100|l'0\rangle W(\tfrac12 1Jl;\tfrac12 l')\left[\frac{p b_{l'}(p_3,p)}{E_p+M} - \frac{p_3 b_l(p_3,p)}{E_{p_3}+M}\right], \tag{3.12}$$

where

$$\begin{aligned} b_l(p_3,p) &= 2\pi\int_{-1}^{1} dz\, P_l(z) b(p_3,p,z) = \frac{2\pi}{pp_3}Q_l(a) ,\\ b(p_3,p,z) &= (\mu^2-t)^{-1} ,\\ z &= \hat p\cdot\hat p_3, \quad a = (2E_pE_{p_3}+\mu^2-2M^2)/2pp_3 , \end{aligned} \tag{3.13a}$$

and

$$C^I_{\epsilon,l'} = 16\pi R_{\epsilon,l'}[3(E_p+M)(E_{p_3}+M)/8M^2]^{1/2}\chi_\epsilon^I g . \tag{3.13b}$$

The dependence of $C^I_{\epsilon,l'}$ on W_3 through E_{p_3} is sufficiently mild that we may consider it constant. From Eq. (2.20) we identify the OPE partial cross section $\sigma_\epsilon^I(J,l',l)$ for the reaction $\pi N\to\epsilon N$ as

$$\sigma_\epsilon^I(J,l',l) = \frac{4\pi}{p^2}(J+\tfrac12)\frac{h(W)}{R_{\epsilon,l'}^{\,2}}\int_{2\mu}^{W-M} p_3 W_3^{\,2} dW_3\,\frac{\sin^2\delta_\epsilon(q_{12})}{q_{12}}|b_\epsilon^I(J,l',l)|^2 v_{l'} . \tag{3.14}$$

We now derive equations similar to the above for the $\pi N\to\rho N$ case: The equation analogous to (2.9) is

$$T_\rho^I = \sum_\lambda \sqrt3\,\chi_\rho^I g\,\frac{\bar u_r(\vec p')\gamma_5 u_s(\vec p)}{\mu^2-t}\,V_\lambda\,\frac{[48\pi W_3 e^{i\delta_\rho(q_{12})}\sin\delta_\rho(q_{12})]}{q_{12}^{\;3}}\,V'_\lambda , \tag{3.15}$$

where χ_ρ^I is obtained from Eq. (3.8). We have chosen to go off-shell by replacing $P_1(z_{\pi\pi})/q_{12}$ in Eq. (3.1) by $\vec V\cdot\vec V'/q_{12}^{\;3}$, where $\vec V(\vec V')$ is the relative momentum of the two pions in their own c.m. system. Thus, in Eq. (3.15) V_λ becomes the spin wave function of the ρ and λ becomes the z component of spin. Aaron, Amado, and Young[20] have shown that in an arbitrary Lorentz frame

$$\vec V = \vec k - \frac{k\cdot K}{K^2}\vec K - \frac{\{[\vec k-(k\cdot K/K^2)\vec K]\cdot\vec K\}}{K_0(K_0+W)}\vec K , \tag{3.16}$$

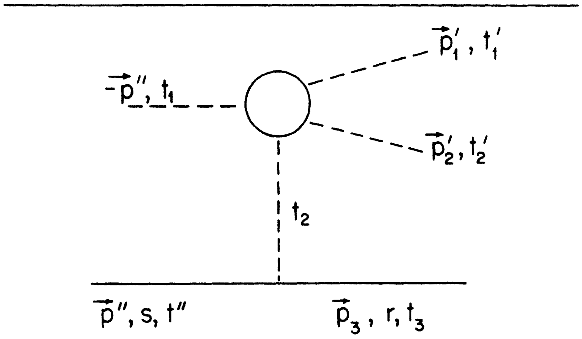

FIG. 1. Schematic representation of one-pion-exchange Born term.

with

$$\begin{aligned} K &= k_1+k_2 ,\\ 2k &= k_1-k_2 ,\\ W^2 &= K^2 ,\\ K_0^{\,2}-K^2 &= \vec K^2 . \end{aligned} \tag{3.17}$$

In Eq. (3.17) k_1 and k_2 are the pion momenta associated with the $\rho\to2\pi$ vertex. For the OPE diagram described by Eq. (3.15), $\vec V$ and $\vec V'$ are

$$\begin{aligned} \vec V &= -\vec p + \left[\frac{\omega_p}{m_\rho} - \frac{\vec p\cdot\vec p_3}{m_\rho(\omega_\rho+m_\rho)}\right]\vec p_3 ,\\ m_\rho^{\,2} &= (P-p_3)^2 ,\\ \omega_\rho &= (\vec p_3^{\,2}+m_\rho^{\,2})^{1/2} , \end{aligned} \tag{3.18}$$

and

$$\vec V' = \tfrac12(\vec p_1-\vec p_2) - \frac12\,\frac{(\vec p_1^{\,2}-\vec p_2^{\,2})}{\omega_\rho(\omega_\rho+m_\rho)}\,\vec p_3 . \tag{3.19}$$

By comparing Eqs. (3.15) and (2.9) we see that

$$\langle\vec p_3 r\lambda|b_\rho^I|\vec p s\rangle = \sqrt3\,\chi_\rho^I\,\frac{48\pi g u_r(p')\gamma_5 u_s(\vec p)}{\mu^2-t}\,V_\lambda . \tag{3.20}$$

In terms of Pauli spinors the above equation may be cast in the form

$$\langle \vec{p}_3 r\lambda | b_\rho^I | \vec{p}s\rangle \equiv a_{pp} p_\lambda \chi_r^\dagger \vec{\sigma}\cdot\vec{p}\chi_s + a_{pp_3} p_\lambda \chi_r^\dagger \vec{\sigma}\cdot\vec{p}_3\chi_s + a_{p_3p} p_{3\lambda}\chi_r^\dagger\vec{\sigma}\cdot\vec{p}\chi_s + a_{p_3p_3} p_{3\lambda}\chi_r^\dagger\vec{\sigma}\cdot\vec{p}_3\chi_s\,, \tag{3.21}$$

with

$$a_{pp} = C_\rho^I \frac{b(p_3,p,z)}{E_p+M}\,,\quad a_{pp_3} = -C_\rho^I \frac{b(p_3,p,z)}{E_{p_3}+M}\,,$$
$$a_{p_3p} = C_\rho^I \frac{b(p_3,p,z)}{E_p+M}\left[\frac{\vec{p}\cdot\vec{p}_3}{m_\rho(\omega_\rho+m_\rho)} - \frac{\omega_p}{m_\rho}\right],\quad a_{p_3p_3} = -C_\rho^I \frac{b(p_3,p,z)}{E_{p_3}+M}\left[\frac{\vec{p}\cdot\vec{p}_3}{m_\rho(\omega_\rho+m_\rho)} - \frac{\omega_\rho}{m_\rho}\right], \tag{3.22}$$

where $b(p_3,p,z)$ is given by Eq. (3.13) and

$$C_\rho^I = 48\pi[3(E_p+M)(E_{p_3}+M)/4M^2]^{1/2}\chi_\rho^I g\,. \tag{3.23}$$

The partial-wave amplitudes are now given by

$$R_{\rho,l'}^{-1}(2v_{l'})^{1/2} b_\rho^I(J,j,l',l) = \sum_{\substack{m,m',m_j\\ r,s}} \int d\Omega_{\hat{p}_3}\int d\Omega_{\hat{p}}\langle l'jm'm_j|JM\rangle\langle\tfrac{1}{2}1r\lambda|jm_j\rangle$$
$$\times Y_{l'm'}^*(\hat{p}_3)\langle\vec{p}_3 r\lambda|b_\rho^I|\vec{p}s\rangle Y_{lm}(\hat{p})\langle l\tfrac{1}{2}ms|JM\rangle\,. \tag{3.24}$$

Using Eq. (3.11) and

$$\vec{p}\cdot\vec{p}_3 = \frac{4\pi}{3} pp_3 \sum_\alpha Y_{1\alpha}^*(\hat{p})Y_{1\alpha}(\hat{p}_3)\,, \tag{3.25}$$

we finally obtain for the partial-wave amplitude

$$R_{\rho,l'}^{-1}(2v_{l'})^{1/2} b_\rho^I(J,j,l',l) = C_\rho^I[6(2l+1)(2l'+1)(2j+1)]^{1/2}(-1)^{3/2-j}$$
$$\times\sum_\Lambda \langle l'100|\Lambda 0\rangle\langle l100|\Lambda 0\rangle\left[\frac{p^2}{E_p+M} b_{l'}(p_3,p) - \frac{pp_3}{E_p+M}\frac{\omega_p}{m_\rho} b_\Lambda(p_3,p)\right.$$
$$+\frac{p^2p_3^{\,2}}{E_p+M}\frac{1}{m_\rho(\omega_\rho+m_\rho)}\sum_\lambda(\langle 1\Lambda 00|\lambda 0\rangle)^2 b_\lambda(p_3,p)$$
$$+\frac{p_3^{\,2}}{E_{p_3}+M}\frac{\omega_p}{m_\rho} b_l(p_3,p)$$
$$\left.-\frac{pp_3^{\,3}}{E_{p_3}+M}\frac{1}{m_\rho(\omega_\rho+m_\rho)}\sum_\lambda(\langle 1l00|\lambda 0\rangle)^2 b_\lambda(p_3,p)\right]$$
$$\times W(\tfrac{1}{2}1Jl';j\Lambda)W(\tfrac{1}{2}1Jl;\tfrac{1}{2}\Lambda) - \frac{pp_3}{E_{p_3}+M} b_\Lambda(p_3,p)\begin{Bmatrix}\Lambda & 1 & l'\\ 1 & \tfrac{1}{2} & j\\ l & \tfrac{1}{2} & J\end{Bmatrix}, \tag{3.26}$$

where

$$\begin{Bmatrix}\Lambda & 1 & l'\\ l & \tfrac{1}{2} & j\\ l & \tfrac{1}{2} & J\end{Bmatrix}$$

is a 9-j symbol.[21] In terms of Eq. (3.26) above the OPE partial cross section $\sigma_\rho^I(J,j,l',l)$ identified from Eq. (2.20) is

$$\sigma_\rho^I(J,j,l',l) = \frac{4\pi}{p^2}\left(J+\frac{1}{2}\right)\frac{h(W)}{3R_{\rho,l'}^{\,2}}\int_{2\mu}^{W-M} p_3W_3^{\,2}dW_3\,\frac{\sin^2\delta_\rho(q_{12})}{q_{12}^{\,3}}\,|b_\rho^I(J,j,l',l)|^2 v_{l'}\,. \tag{3.27}$$

In calculations of σ_ϵ^I and σ_ρ^I [Eqs. (3.14) and (3.27), respectively] the normalization factors R appear in the Born terms b_ϵ^I and b_ρ^I, and thus cancel from the equations.

IV. CALCULATIONS AND DISCUSSION

We have programmed Eqs. (3.14) and (3.27) and evaluated the partial-wave cross sections in the energy range 1300 to 2200 MeV. The above calculations include as input the $I=0$, $J=0$ (ϵ) and $I=1$, $J=1$ (ρ) $\pi\pi$ phase-shift analysis given by recent data analyses.[22] Because of uncertainties in

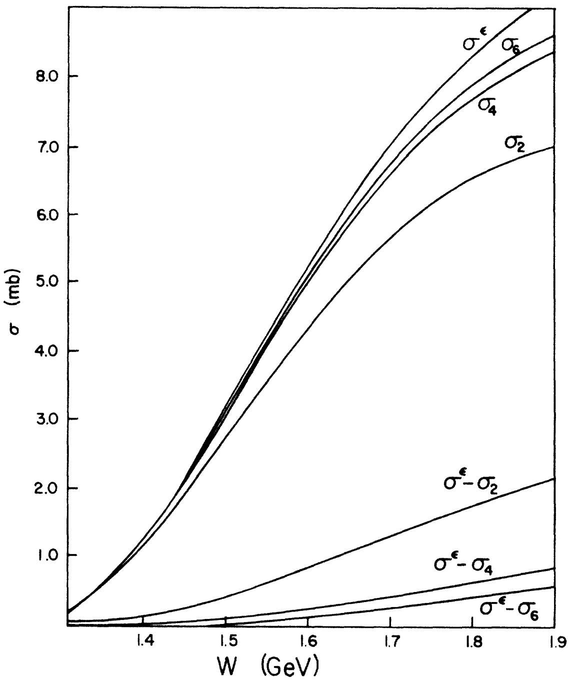

FIG. 2. Total "ϵ" cross section and partial sums vs total center-of-mass energy W.

the ϵ phase around $K\bar{K}$ threshold, we only give the $\pi N \to \epsilon N$ results up to 1900 MeV. In Fig. 2 we give the total $I=\frac{1}{2}$ $\pi N \to \epsilon N$ cross section σ^ϵ as a function of overall center-of-mass energy W. In Fig.

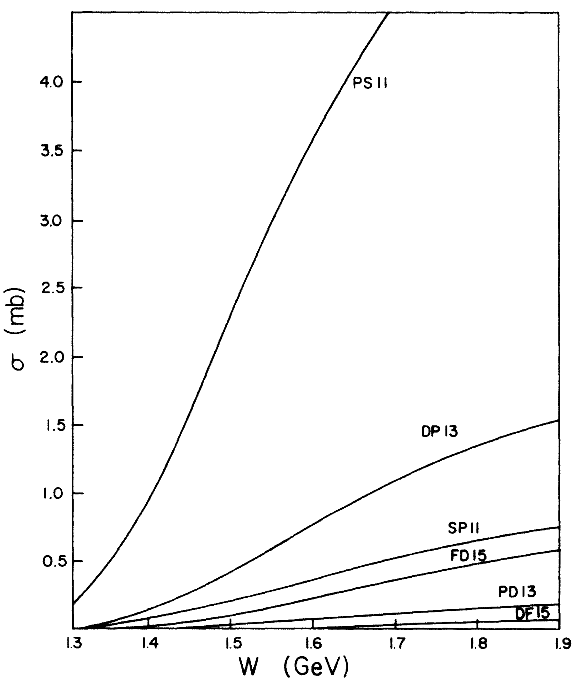

FIG. 3. Partial-wave "ϵ" cross sections vs total center-of-mass energy W.

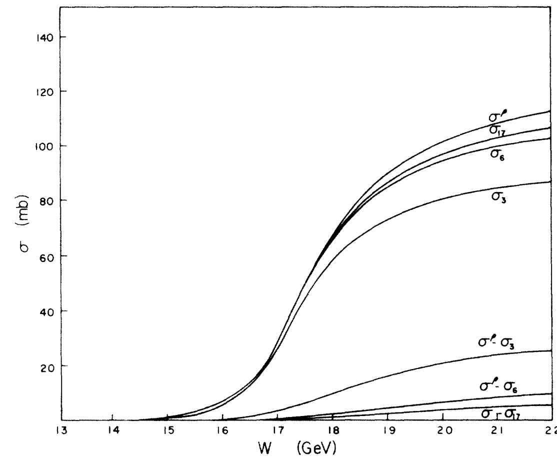

FIG. 4. Total "ρ" cross section and partial sums vs total center-of-mass energy W.

3 we give the partial-wave ϵN cross sections for the six ϵ waves chosen for initial inclusion in the BSC fit. In Fig. 2 we also give $\sigma^\epsilon - \sigma_2$, $\sigma^\epsilon - \sigma_4$, and $\sigma^\epsilon - \sigma_6$, where σ_2, σ_4, and σ_6 are the sums of the two, four, and six largest partial-wave cross sections. In Fig. 4 we give the total $I=\frac{1}{2}$ $\pi N \to \rho N$ cross sections σ^ρ. In Fig. 5 we give the three largest ρN partial-wave cross sections, and in Fig. 6 we show 14 additional ones. The 17 cross sections chosen were, again, those selected for initial inclusion in the BSC fit. In Fig. 4 we also show (for the case of ρ production) σ_3, σ_6, σ_{17}, $\sigma^\rho - \sigma_3$, $\sigma^\rho - \sigma_6$, and $\sigma^\rho - \sigma_{17}$. Finally in Fig. 7 we show on an enlarged scale $\sigma^\rho - \sigma_3$, $\sigma^\rho - \sigma_6$, and $\sigma^\rho - \sigma_{17}$.

The contributions shown in Figs. 4–7 are for $I=\frac{1}{2}$; the $I=\frac{3}{2}$ cross sections are obtained by mul-

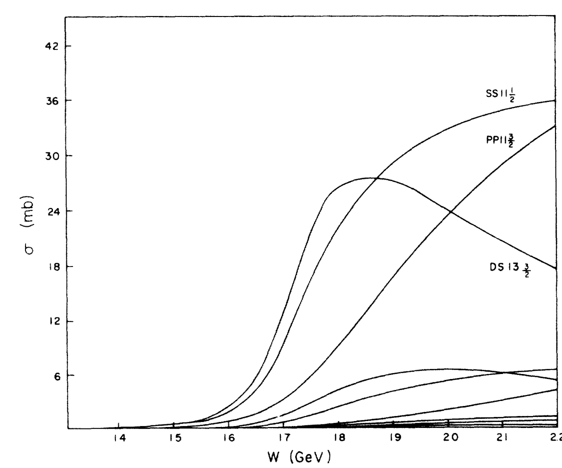

FIG. 5. Three largest partial-wave "ρ" cross sections (labeled) vs total center-of-mass energy W. The unlabeled curves are shown in detail using an expanded scale in Fig. 6.

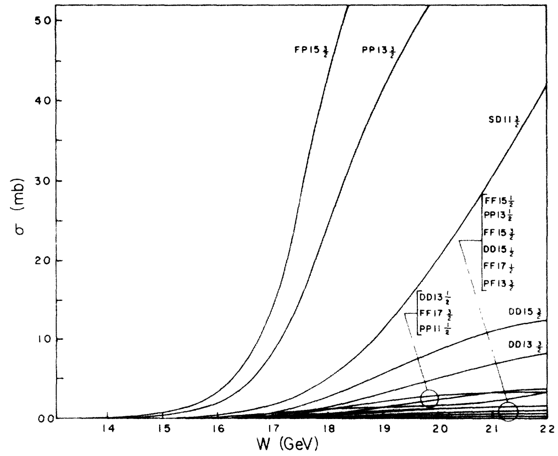

FIG. 6. Partial-wave "ρ" cross sections vs total center-of-mass energy W.

tiplying the $I=\frac{1}{2}$ ones by $\frac{1}{4}$. For the three processes

$$\pi^- p \to \pi^+\pi^- n\,,$$
$$\pi^- p \to \pi^-\pi^0 p\,,$$
$$\pi^+ p \to \pi^+\pi^0 p\,,$$

the ρ cross-section contributions are found from the figures by multiplying by $\frac{1}{4}$, $\frac{1}{8}$, and $\frac{1}{8}$. The ϵ contributions to $\pi^- p \to \pi^+\pi^- n$ are found by multiplying the curves in Figs. 2 and 3 by $\frac{2}{9}$.

The unitarity limit at $W=2.0$ GeV is about $(J+\frac{1}{2})\times 2$ mb. One sees that the three largest ρN partial waves $SS11_{1/2}$, $PP11_{3/2}$, and $DS13_{3/2}$ violate the limit badly. Pion-nucleon dynamics must modify those partial waves substantially, but one expects them to remain important. The first and last are indeed important in the BSC fit, *but the second is not kept. The $PP13_{3/2}$ partial wave, large in Fig. 6, is also omitted in the BSC fit.* Instead, of these partial waves, they include in their final fit the channel-spin-$\frac{1}{2}$ partial waves $PP11_{1/2}$ and $PP13_{1/2}$ which are small in Fig. 6. It should be noted that another (Saclay) $\pi N \to \pi\pi N$ analysis[23] disagrees with the absence of channel spin $j=\frac{3}{2}$ ρ found in the BSC fit. The absence of the $j=\frac{3}{2}$ P-wave coupling in the BSC fit motivated speculation by Faiman[24] of suppression of the longitudinal ρ-N coupling, later abandoned[25] in view of the Saclay result. One would expect the OPE calculations to be definitive on the channel-spin $\frac{1}{2}$ vs $\frac{3}{2}$ question since it is difficult to imagine any known dynamical mechanism inverting such large ratios as those in Figs. 5 and 6. The major OPE partial wave not included by BSC is the $GD17_{3/2}$, its cross section reaching 40% of the unitarity limit at ~2 GeV, and thus accounting for about 80% of $\sigma^\rho - \sigma_{17}$. The partial-wave cross sections of Figs. 5 and 6 may be compared with the results of Amaldi and Selleri.[10] These authors compute the sum over ρN states for given J (up to and including G waves) both for the one-pion-exchange diagram considered here and for a unitarized modification. Their sums agree with ours when comparable.

Since Eq. (3.26) is rather complicated we checked it for the four $PP1J_j$ ρ waves in the helicity formalism using the OPE formulas of Gasiorowicz[26] in the parity-conserving, partial-wave helicity amplitudes of GGLMZ,[27] and then coupling these together to form L-S amplitudes by the prescription of Herndon *et al.* We obtain directly the result (k is the πN relative momentum; q is the ρN relative momentum)

$$F_j^J=\frac{k}{E_k+M}\sum_{l=0}^{3}C_{k,l}Q_l(a)+\frac{q}{E_q+M}\sum_{l=0}^{3}C_{q,l}Q_l(a)\,, \tag{4.1}$$

$$a=(2M^2-\mu^2-2E_kE_q+k^2+q^2)/2kq\,,$$

where $C_{k,l}$ and $C_{q,l}$ are given in Table I. Equation (4.1) agrees with Eq. (3.26) when the Clebsch-Gordan coefficients, Racah coefficients, and 9-j symbols are replaced by their algebraic forms in the latter equation.

Our results have important implications for $\pi\pi N$ analyses. The cross sections of Figs. 2–7 may be compared with the experimental cross sections. These are shown in Ref. 5, and in the energy region 1.5 to 2.0 GeV, the $n\pi^-\pi^+$, $p\pi^-\pi^0$, and $n\pi^+\pi^0$ cross sections are roughly 8 mb, 5 mb, and 9 mb, respectively. One can see from the above figures that $\sigma^\epsilon - \sigma_6$ and $\sigma^\rho - \sigma_{17}$ contribute 10 to 15% of these cross sections at the high end of the range. In view of these results we suggest that a sensible

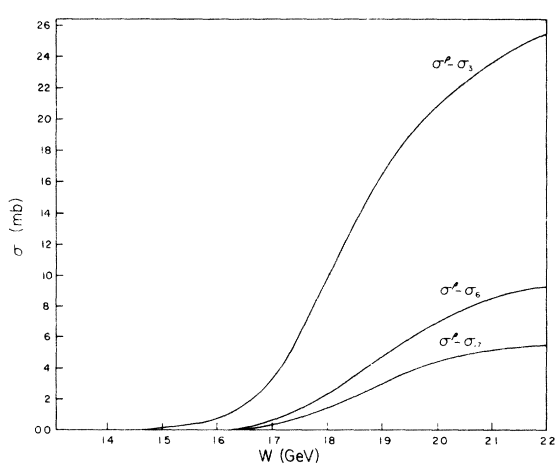

FIG. 7. "ρ" cross-section differences vs total center-of-mass energy W.

TABLE I. Coefficients of the Legendre functions of the second kind in the helicity decomposition of the $I=\frac{1}{2}$, $l=1$, $l'=1$ partial waves.

	$J=\frac{1}{2}, j=\frac{3}{2}$	$J=\frac{3}{2}, j=\frac{3}{2}$	$J=\frac{1}{2}, j=\frac{1}{2}$	$J=\frac{3}{2}, j=\frac{1}{2}$
$Q_3\frac{k}{E_k+M}$	0	$\frac{\sqrt{10}}{30}(\omega-m_\rho)$	0	$\frac{1}{30}(\omega-m_\rho)$
$Q_3\frac{q}{E_q+M}$	0	0	0	0
$Q_2\frac{k}{E_k+M}$	0	$-\frac{\sqrt{10}}{18}q$	0	$-q/18$
$Q_2\frac{q}{E_q+M}$	$\frac{1}{54}(2\omega-m_\rho)$	$\frac{\sqrt{10}}{27}(2m_\rho-\omega)$	$\frac{1}{27}(\omega+m_\rho)$	$\frac{1}{54}(m_\rho-\omega)$
$Q_1\frac{k}{E_k+M}$	$-\omega/18$	$\frac{\sqrt{10}}{90}(3m_\rho+2\omega)$	$\omega/18$	$\frac{1}{90}(3m_\rho+2\omega)$
$Q_1\frac{q}{E_q+M}$	$-q/18$	$\frac{\sqrt{10}}{18}q$	$q/18$	$q/18$
$Q_0\frac{k}{E_k+M}$	$q/18$	0	$-q/18$	0
$Q_0\frac{q}{E_q+M}$	$\frac{1}{54}(\omega+m_\rho)$	$\frac{\sqrt{10}}{54}(\omega+4m_\rho)$	$\frac{1}{54}(2m_\rho-\omega)$	$\frac{1}{54}(\omega+m_\rho)$

procedure in fitting $\pi N\to\pi\pi N$ would be to add to the partial waves whose amplitudes are being varied a background term made up of the remainder of the two one-pion-exchange diagrams ($\pi N\to\epsilon N$ and $\pi N\to\rho N$). The $GD17$ wave is so large that we would probably include it among the waves being varied. (Alternatively, one could estimate absorptive corrections by the methods of the Appendix.) Because the phase of this background is known, one can determine in terms of it the phases of the ϵN, ρN, $\pi\Delta$, etc., partial-wave isobar amplitudes. Since even without the $GD17$ were the OPE background contributes 2 to 3% of the cross section, it can easily contribute a considerably higher percentage of the amplitude, and thus could provide a reliable standard against which to measure partial-wave isobar amplitude phases. By comparison, the BSC analysis determined the same phases by following energy-independent partial-wave isobar-model $\pi N\to\pi\pi N$ fits with simultaneously-coupled-channel, energy-dependent K-matrix fits to the elastic and isobar amplitudes. In addition to the BSC analysis discussed above, there are also detailed partial-wave analyses by a Saclay group mentioned earlier[23] and an Imperial College[28] group. The results of all three analyses were recently summarized by Barnhum[29] and their ρN results were compared to a preliminary calculation[30] of our six most important ρN partial waves. We reproduce here in Table II Barnhum's ρN wave comparison.

Another important reason for including peripheral OPE in fitting is the sizable angular dependence it is capable of generating. Even when it is responsible for a small fraction of the cross section we have found that in some regions of phase space it can dominate the amplitude. Also, recent work has indicated that OPE with $I=2$ $\pi\pi$ contributions

TABLE II. Comparison between OPE (ρN) cross-section predictions and the corresponding results of phase-shift analyses. For each I, we list the six largest partial waves. The symbols used and their meanings are: X, not found to be necessary; F, found at a number of energies; S, strong enough to determine signs.

Theory	Experiment		
This paper	Berkeley-SLAC	Saclay	Imperial College
$I=\frac{1}{2}$			
(1) $DS13_{3/2}$	S	S	
(2) $SS11_{1/2}$	F	F	
(3) $PP11_{3/2}$	X	S	
(4) $FP15_{3/2}$	S	S	
(5) $PP13_{3/2}$	X	F	
(6) $SD11_{3/2}$	X	S	
$I=\frac{3}{2}$			
(1) $DS33_{3/2}$	F	F	F
(2) $SS31_{1/2}$	F	F	S
(3) $PP31_{3/2}$	X	F	F
(4) $FP35_{3/2}$	S	X	F
(5) $PP33_{3/2}$	X	F	F
(6) $SD31_{3/2}$	X	F	F

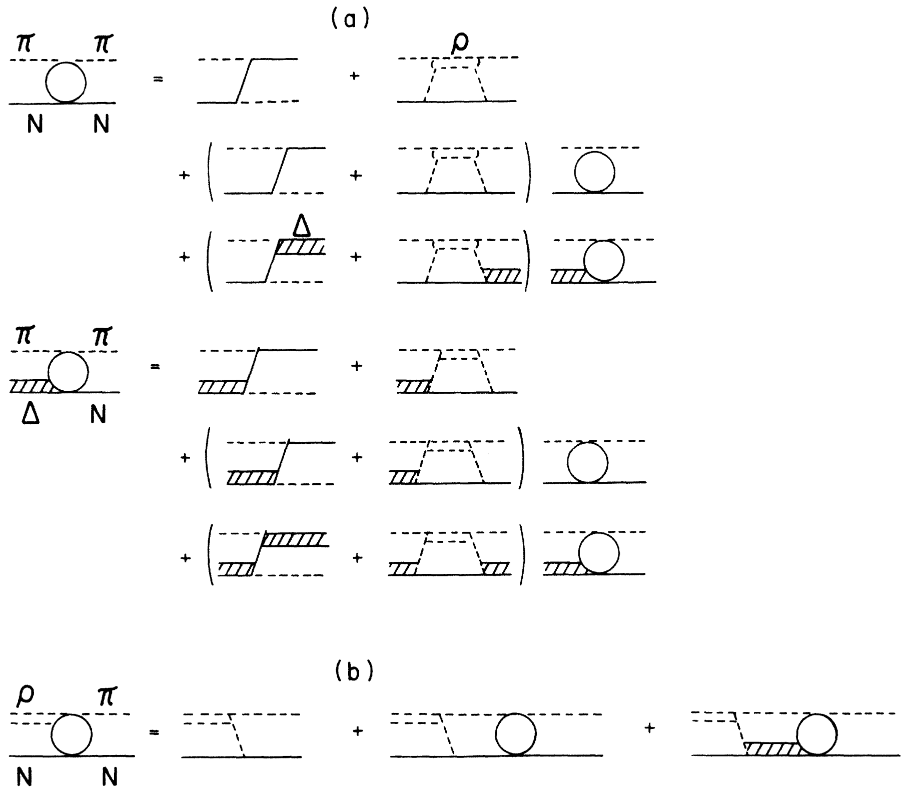

FIG. 8. (a) Coupled integral equations for $\pi N \rightarrow \pi N$ and $\pi N \rightarrow \pi\Delta$. (b) Integral relation for obtaining $\rho N \rightarrow \pi N$ amplitude from solutions of integral equations shown in (a).

may be important.[23,28] We believe that fits neglecting peripheral OPE are suspect. The procedure recommended of including peripheral OPE is, of course, analogous to that used in fitting nucleon-nucleon scattering. We are in the process of trying it in the $\pi N \rightarrow \pi\pi N$ problem and hope to report on the results in due course.

Note added. After completion of this paper we were informed of a study (unpublished) by D. Novoseller of the effects of OPE on the isobar analysis of $\pi N \rightarrow \pi\pi N$. He has made significant progress on the problem, and we are grateful to him for enlightening conversations concerning his research.

APPENDIX: UNITARIZED ISOBAR AMPLITUDES

We have performed preliminary studies of unitarization and subenergy dependence of isobar amplitudes using (unpublished) information contained in earlier elastic πN calculations by Aaron and Amado (AA).[31] In particular, we have examined the isobar amplitudes for production of ρ and Δ states that connect to an initial πN D_{13} state at total c.m. energy $W = 1520$ MeV. (The ϵN state which is produced in a P wave from the initial D_{13} state was found to be relatively unimportant at this energy.) These amplitudes were obtained using a dynamical scheme that incorporates analyticity and three-body unitarity, and the results obtained for the elastic D_{13} amplitudes were in reasonable agreement with experiment for energies 1400 MeV $\lesssim W \lesssim$ 2000 MeV.[31] The coupled integral equations shown schematically in Fig. 8(a) were solved numerically to obtain half off-shell amplitudes for the processes $\pi N \rightarrow \pi N$ and $\pi N \rightarrow \pi\Delta$. The $\pi N \rightarrow \rho N$ amplitudes were then obtained by integrals over the previous amplitudes as shown in Fig. 8(b). The $DS13_{3/2}$ ρN isobar amplitude is shown in Fig. 9 (see Ref. 32) along with the corresponding Born term given by Eq. (3.26). In Fig. 10 (see Ref. 32) we show the AA $\pi\Delta$ $DS13$ and $DD13$ amplitudes. There are several interesting features to note in the above figures:

(1) The $DS13_{3/2}$ ρN amplitude is remarkably constant as a function of subenergy, much more so than the Born term itself. It is essentially pure imaginary as is the BSC solution, but smaller than the latter. Note the linearity of the Born term as a function of q^2 (where q is the relative momentum in the isobar c.m. system).

(2) The $DS13$ $\pi\Delta$ amplitude is a rapidly varying

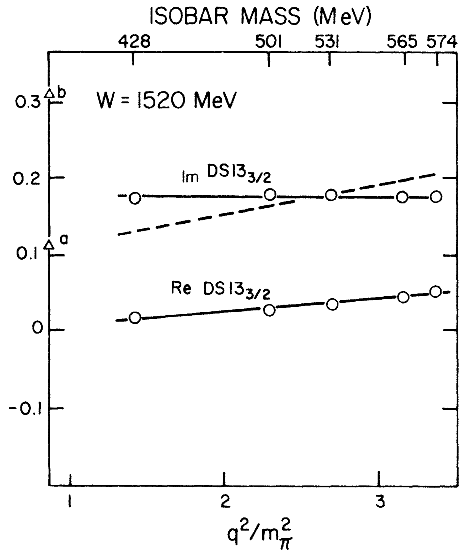

FIG. 9. Isobar amplitudes for production of ρN (channel spin $\frac{3}{2}$) through the $D13$ πN partial wave vs q^2 (q is the three-momentum in the π-π c.m. system) at total c.m. energy $W = 1520$ MeV. The isobar mass is given on the upper scale. The straight lines are interpolations of the theoretical points shown as black dots. The corresponding Berkeley-SLAC amplitude $DS13_{3/2} = 0.114 + 0.315\,i \equiv a + ib$ is indicated on the graph. The dashed curve shows the Born term given by Eq. (3.26) of the text.

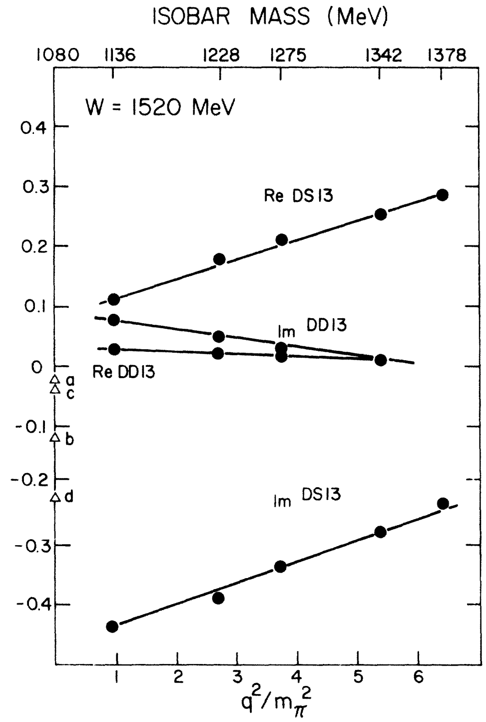

FIG. 10. Isobar amplitudes for production of $\pi\Delta$ through the $D13$ πN partial wave vs q^2 (q is the three-momentum in the Δ c.m. system) at total c.m. energy $W = 1520$ MeV. The isobar mass is given on the upper scale. The straight lines are interpolations of the theoretical points shown as black dots. The corresponding Berkeley-SLAC amplitudes (independent of q^2) are $DS13(\Delta) = 0.026 - 0.120\,i \equiv a + ib$, and $DD13(\Delta) = -0.042 - 0.226\,i \equiv c + id$, and are indicated on the graph.

function of subenergy. The linear dependence on q^2 is striking and was suggested in a previous paper.[6]

(3) The $DD13$ $\pi\Delta$ amplitude of AA is near zero and is thus inconsistent with BSC. The AA result seems reasonable in view of the ranges of the forces involved, the nearness to $\pi\Delta$ threshold, and the fact that all obvious Feynman diagrams enhance S-wave production relative to D-wave production of $\pi\Delta$ near threshold. It is possible that strong, very-short-range (quark?) interactions not included in the AA calculation make the $DD13$ $\pi\Delta$ behave in the manner obtained by BSC, but it is more likely that their large D-wave amplitude is an artifact of their model, particularly their neglect of unitarity.

The above results indicate that the subenergy dependence of isobar amplitudes may be studied in available dynamical models. Furthermore, even though the subenergy dependence of these amplitudes may be considerable, it may also be of a simple functional form (i.e., linear in q^2) and thus may be treated relatively easily in data analyses.

---

†Work supported in part by the National Science Foundation.

*Work supported in part by the Energy Research and Development Administration.

[1]H. J. Melosh, Phys. Rev. D 9, 1095 (1974).

[2]F. J. Gilman, M. Kugler, and S. Meshkov, Phys. Rev. D 9, 715 (1974).

[3]D. Faiman and J. Rosner, Phys. Lett. 45B, 357 (1973).

[4]D. J. Herndon, R. S. Longacre, L. R. Miller, A. H. Rosenfeld, G. Smadja, P. Söding, R. J. Cashmore, and D. W. G. S. Leith, Phys. Rev. D 11, 3183 (1975). Hereafter referred to as BSC.

[5]D. J. Herndon, P. Söding, and R. J. Cashmore, Phys. Rev. D 11, 3165 (1975). Our formulation follows more closely that of Y. Goradia and T. A. Lasinski, *ibid.* 15, 220 (1977). See also B. H. Bransden and R. G. Moorhouse, *The Pion-Nucleon System* (Princeton Univ. Press., Princeton, New Jersey, 1973). These authors suggest the following earlier references: R. M. Sternheimer and S. J. Lindenbaum, Phys. Rev. 123, 333

(1961); D. Z. Freedman, C. Lovelace, and J. M. Namylslowski, Nuovo Cimento A43A, 218 (1966); M. C. Olsson and G. B. Yodh, Phys. Rev. 145, 1309 (1966); D. Morgan, *ibid.* 166, 1731 (1968); J. M. Namylslowski, M. S. K. Razmi, and R. G. Roberts, *ibid.* 157, 1328 (1967); R. J. Glauber, in *Lectures in Theoretical Physics*, edited by W. E. Brittin and L. G. Dunham (Interscience, New York, 1959), Vol. I.

[6]R. Aaron and R. D. Amado, Phys. Rev. Lett. 31, 1157 (1973).

[7]R. Aaron and R. D. Amado, Phys. Rev. D 13, 2581 (1976).

[8]R. Longacre and R. Aaron, Phys. Rev. Lett. 38, 1509 (1977).

[9]G. F. Chew and F. E. Low, Phys. Rev. 113, 1640 (1959).

[10]For example, an early application of the Chew-Low suggestion was made by L. S. Rodberg, Phys. Rev. Lett. 3, 58 (1959), to deduce the low-energy $\pi\pi$ amplitude from $\pi N \rightarrow \pi\pi N$ data near threshold. A much more detailed discussion of OPE effects in $\pi N \rightarrow \pi\pi N$ is given by U. Amaldi and F. Selleri, Nuovo Cimento 31, 360 (1964). For a more complete bibliography see J. D. Jackson, Rev. Mod. Phys. 37, 484 (1965).

[11]See for example M. J. Moravcsik, in *Dispersion Relations*, edited by G. R. Screaton (Interscience, Edinburgh, Scotland, 1961), pp. 117–165.

[12]H. Pilkuhn, *The Interactions of Hadrons* (Wiley, New York, 1967).

[13]J. D. Bjorken and S. D. Drell, *Relativistic Quantum Mechanics* (McGraw-Hill, New York, 1964).

[14]See Appendix B of Ref. 13.

[15]Our Clebsch-Gordan and Racah coefficients are defined in M. E. Rose, *Elementary Theory of Angular Momentum* (Wiley, New York, 1957).

[16]R. Aaron, *Modern Three-Hadron Physics*, edited by A. W. Thomas (Springer, Heidelberg, W. Germany, 1976), Chap. 5.

[17]J. M. Blatt and V. F. Weisskopf, *Theoretical Nuclear Physics* (Wiley, New York, 1952), p. 361.

[18]Y. Goradia, Phys. Rev. D 15, 1368 (1977).

[19]See Ref. 15, p. 85.

[20]R. Aaron, R. D. Amado, and J. E. Young, Phys. Rev. 174, 2022 (1968).

[21]A. R. Edmonds, *Angular Momentum in Quantum Mechanics* (Princeton Univ. Press, Princeton, New Jersey, 1957).

[22]P. Nath, in *Experimental Meson Spectroscopy—1974*, proceedings of the Boston Conference, edited by D. A. Garelick (AIP, New York, 1974), p. 192

[23]J. Dolbeau, M. Neveu, F. A. Triantis, and F. Cadiet (unpublished); R. S. Longacre and J. Dolbeau (unpublished).

[24]D. Faiman, Phys. Lett. 49B, 365 (1974).

[25]D. Faiman, Weismann Institute of Science Report No. W1S-75/53-Ph (unpublished).

[26]S. Gasiorowicz, *Elementary Particle Physics* (Wiley, New York, 1967), pp. 462–465.

[27]M. Gell-Mann, M. L. Goldberger, F. E. Low, E. Marx, and F. Zachariasen, Phys. Rev. 133, B145 (1964). This paper is conventionally referred to as GGLMZ.

[28]I. Butterworth and K. W. J. Branhum, private communication.

[29]K. W. J. Barnhum, Invited talk presented at the Topical Conference on Baryon Resonances, Oxford, 1976 (unpublished).

[30]Y. Goradia and V. L. Teplitz, work presented at the conference of Ref. 29. The graphs in this work contained an error in scale which has been corrected in the present paper.

[31]R. Aaron and R. D. Amado, Phys. Rev. Lett. 27, 1316 (1971).

[32]An incorrect version of this diagram appeared in Ref. 7. The amplitudes shown there contained extraneous kinematical factors.